DNA Manipulation and Separation in Sublithographic-Scale Nanowire Array

Takao Yasui,[†,*] Sakon Rahong,[‡] Koki Motoyama,[†,▲] Takeshi Yanagida,[‡,*] Qiong Wu,[†] Noritada Kaji,[†] Masaki Kanai,[‡] Kentaro Doi,[§] Kazuki Nagashima,[‡] Manabu Tokeshi,[†,⊥] Masateru Taniguchi,[‡] Satoyuki Kawano,[§] Tomoji Kawai,[‡,*] and Yoshinobu Baba[†,∥,*]

[†]Department of Applied Chemistry, Graduate School of Engineering, Nagoya University, and FIRST Research Center for Innovative Nanobiodevices, Nagoya University, Furo-cho, Chikusa-ku, Nagoya 464-8603, Japan, [‡]Institute of Scientific and Industrial Research, Osaka University, 8-1 Mihogaoka Ibaraki Osaka 567-0047, Japan, [§]Department of Mechanical Science and Bioengineering, Graduate School of Engineering Science, Osaka University, Machikaneyama-cho 1-3, Toyonaka, Osaka 560-8531, Japan, [⊥]Division of Biotechnology and Macromolecular Chemistry, Faculty of Engineering, Hokkaido University, Kita 13 Nishi 8, Kita-ku, Sapporo 060-8628, Japan, and [∥]Health Research Institute, National Institute of Advanced Industrial Science and Technology (AIST), Takamatsu 761-0395, Japan. [▲]Current address: Ogawa & Co., Ltd., Nihonbashi Honcho 4-1-11, Chuo-ku, Tokyo 103-0023, Japan.

ABSTRACT Electrokinetic manipulations of biomolecules using artificial nanostructures within microchannels have proven capability for controlling the dynamics of biomolecules. Because there is an inherent spatial size limitation to lithographic technology, especially for nanostructures with a small diameter and high aspect ratio, manipulating a single small biomolecule such as in DNA elongation before nanopore sequencing is still troublesome. Here we show the feasibility for self-assembly of a nanowire array embedded in a microchannel on a fused silica substrate as a means to manipulate the dynamics of a single long T4-DNA molecule and also separate DNA molecules. High-resolution optical microscopy measurements are used to clarify the presence of fully elongated T4-DNA molecules in the nanowire array. The spatial controllability of sublithographic-scale nanowires within microchannels offers a flexible platform not only for manipulating and separating long DNA molecules but also for integrating with other nanostructures to detect biomolecules in methods such as nanopore sequencing.

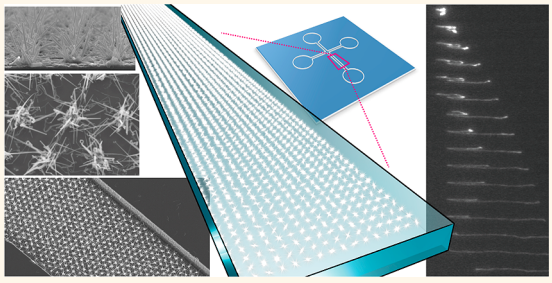

KEYWORDS: nanowire array · nanobiodevices · electrokinetic manipulations · DNA dynamics · DNA separation

Nanobiodevices based on advanced nanotechnologies are opening up a novel research field for biomolecule analysis with ultrahigh resolution, including analysis of single biomolecules. Among the nanotechnologies, an electrokinetic operation of biomolecules by utilizing artificial nanostructures within microfluidics has emerged as a promising analysis technique since it was first proposed. A number of unique artificial nanostructures, such as nanopillar arrays,[1−4] nanowall arrays,[5] nanofilter arrays,[6−9] nanofence arrays,[10] nanochannels,[11−13] and nanoparticles,[14−17] have been examined to control the dynamics of biomolecules. These highly ordered nanostructures have proved less time-intensive to operate and require fewer manual operations when compared with other conventional control methods. Several comprehensive overviews of recent technological, theoretical, and practical developments of nanobiodevices have been made.[18−21]

Although recent progress in micro- and nanofabrication technologies has allowed fabrication of smaller and more precise artificial nanostructures for manipulating biomolecules, there is still an inherent size limitation for lithographic technology. Exploring methodologies to fabricate small and inexpensive nanostructures within microchannels is clearly important to solve the above issues regarding artificial nanostructures for biomolecule manipulations related to single molecule analysis, such as nanopore sequencing.[22,23] Very recently the use of self-assembled ZnO nanowires was proposed as a small nanostructure medium within a microchannel.[24] However the knowledge related to the feasibility of such nanowires for biomolecule manipulations and separations is still not comprehensive due to the difficulties of fabricating

* Address correspondence to (T. Yasui) yasui@apchem.nagoya-u.ac.jp; (T. Yanagida) yanagi32@sanken.osaka-u.ac.jp; (T. Kawai) kawai@sanken.osaka-u.ac.jp; (Y. Baba) babaymtt@apchem.nagoya-u.ac.jp.

Received for review August 27, 2012 and accepted March 13, 2013.

Published online March 13, 2013
10.1021/nn4002424

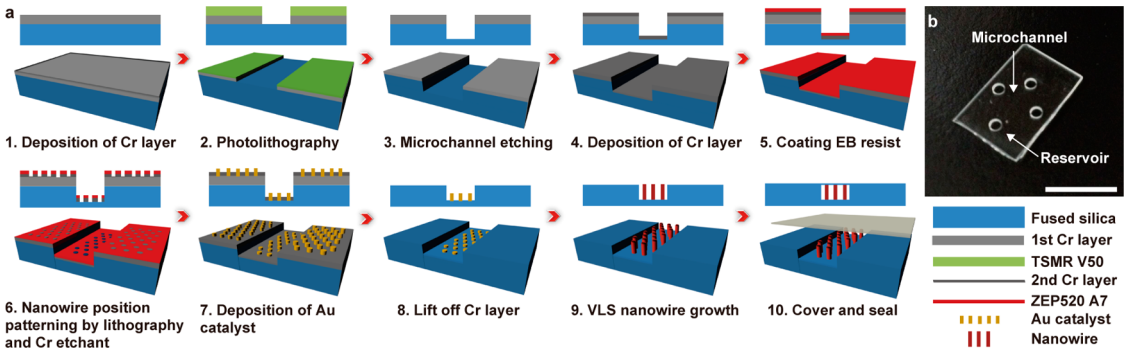

Figure 1. (a) Schematic of the fabrication procedure for self-assembled nanowires embedded in a microchannel. The microchannel and spatially controlled nanowires are formed on a fused silica substrate by utilizing lithographic techniques. (b) Photograph of a fabricated chip with the nanowires embedded in the microchannel; scale bar, 1 cm.

well-defined nanowires within microchannels. Although ideas for the spatial control of nanowires to get a regular array have been extensively studied,[25−31] the use of such precisely positioned nanowire array structures for biomolecule manipulations and separations has not been demonstrated; it is anticipated that the spatially controlled nanowires play an important role in controlling the dynamics of biomolecules and separating them.[18−21]

In this study, we demonstrate the feasibility of using a bottom-up nanowire array structure embedded in microchannels on a fused silica substrate to control the dynamics of long T4-DNA molecules. Compared with a conventional gel sieving matrix or other nanostructures, the nanowire array structure has several advantages, including its capability to fabricate very small objects, which are beyond the size limitation of top-down lithography, its inexpensive fabrication process, and its feasibility to fabricate arbitrary spatial patterns, such as a spot-array pattern. The nanowire is thin enough to elongate DNA molecules effectively with minimal bending deformation, because the nanowire has a radius of less than 100 nm, which is commensurate with the Kuhn length of DNA, 106 nm,[32] and that makes it suitable for efficient DNA elongation from a polymeric perspective. The newly developed nanowire array, which is spatially controlled within microchannels, offers a novel, inexpensive, and flexible platform to manipulate and separate biomolecules.

RESULTS AND DISCUSSION

Nanowire Spot-Array Structure Fabrication. We fabricated the nanowire spot-array structure embedded in the microchannels by utilizing a newly developed self-assembly method (Figure 1a). In this method, the spatial controllability of nanowires can be accomplished by defining the spatial position of metal catalysts only within a microchannel *via* a lift-off process with different thicknesses of Cr layers (Figure 1a-7 and a-8). The Cr layer thickness inside the microchannel is intentionally controlled to be much thinner than that outside the microchannel, which allows us to keep the metal catalysts only within the microchannel during the lift-off process of the Cr layer.

The nanowire chips were fabricated on fused silica substrates (Figure 1b). This was because the Si substrate with a SiO_2 surface layer (having a thickness ranging typically from 50 to 500 nm) exhibited a detrimental dielectric breakdown when applying the relatively high electric voltage (over 100 V) required to cause electrokinetic motion of DNA molecules. (See the example in Figure S1 of the Supporting Information.) A SiO_2 layer, which acted as an adhesion layer when used for sealing with a fused silica cover plate, was deposited as a shell layer on the nanowire surface by sputtering. The shell layer also generates a negatively charged surface on the nanowires, which is essential to avoid the detrimental adhesion of negatively charged DNA. Although choice of the actual appropriate shell material depends on the pH condition of the solvents employed, use of the shell layer allows us to control the surface charge of the nanostructures by considering the isoelectric point of the shell material used. The two major reasons why we used SnO_2 nanowires as the core material are as follows: (i) it is intrinsically difficult to control formation and growth of surface oxides on conventional semiconductor nanowires, including group III−V nanowires, when the wires are exposed to atmospheric conditions and immersed into a liquid; and (ii) other oxide nanowires, such as ZnO and MgO, easily react with surrounding water molecules *via* formation of hydroxides, even in the presence of the SiO_2 shell layer.

Figure 2a shows a schematic of the fabricated chip. Within the microchannel with a width of 25 μm (Figure 2b), the nanowire structure is spot-arrayed with 300 nm in spot diameter and 500 nm in spacing between spots (Figures 2c−e). The nanowire position is well controlled, and the nanowires are self-assembled only within the microchannel. A transmission electron microscope (TEM) image of the nanowires in Figure 2f shows the fabricated nanowire consists of one Au catalyst (10 nm diameter), the SnO_2 single crystalline nanowire (10 nm diameter), and an amorphous

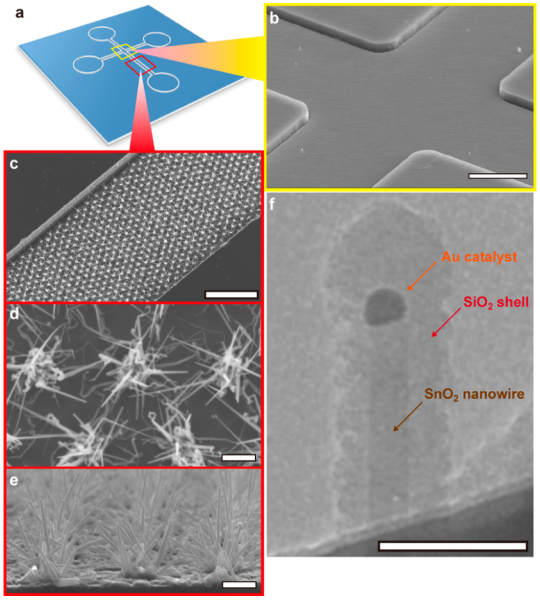

Figure 2. (a) Schematic of fabricated chip. (b) Field emission scanning electron microscope (FESEM) image of the cross-point of the fabricated chip; scale bar, 10 μm. (c) FESEM image of the fabricated nanowire spot-array; scale bar, 10 μm. (d) Magnified FESEM image of the fabricated nanowire spot-array; scale bar, 1 μm. (e) Vertical cross-sectional FESEM image of the fabricated nanowire spot-array; scale bar, 1 μm. (f) Transmission electron microscope (TEM) image of a fabricated nanowire; scale bar, 50 nm.

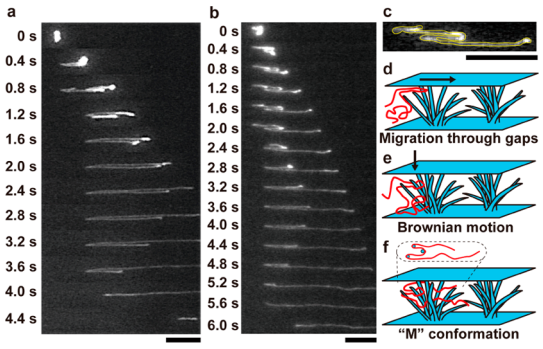

Figure 3. (a) Time-course observations of a T4-DNA molecule in the nanowire spot-array structure under the applied electric field of 10 V/cm; scale bar, 10 μm. (b) Time-course observations of a T4-DNA molecule in the nanowire spot-array structure under the applied electric field of 10 V/cm; scale bar, 10 μm. The T4-DNA molecule shows the characteristic "M"-shaped conformation from 0.8 to 2.0 s. (c) "M"-shaped conformation in the nanowire spot-array structure; scale bar, 10 μm. The outline of the DNA molecule is highlighted as the yellow line. The image is the magnified image at 1.6 s in (b). (d–f) Schematic illustrations showing formation of the "M"-shaped conformation in the nanowire spot-array structure: (d) a DNA molecule migrates through gaps between the nanowires and the cover plate; (e) the migrating DNA molecule settles into the nanowire array structure by Brownian motion; (f) the DNA molecule, now with the "M"-shaped conformation (presented as a top view inside the dotted oval), is entangled with the nanowire array structure.

SiO_2 layer (10 nm thick). The SnO_2 single crystalline nanowire is uniformly covered by the amorphous SiO_2 layer.

DNA Manipulation. Figure 3 shows the observed dynamics of a T4-DNA molecule when colliding with the nanowire spot-array. T4-DNA is fully elongated by the collision with the nanowire spot-array structure, as seen in Figure 3a and Supporting Movie 1. This highlights the potential ability of the nanowire spot-array to control and separate long DNA molecules. The maximum elongation of a T4-DNA molecule was 56.5 μm, which is about 81% of the contour length.[33−35] The contour length of a T4-DNA molecule will be increased by around 23% in our dye-to-base pair ratio (1:5), leading to an extended contour length of 69.4 μm. The T4-DNA molecule inside the nanowire spot-array structure shows typical migration behaviors, including collision, elongation, and contraction. When observing the dynamics of DNA in nanowire arrays, we found a unique behavior for DNA, which has not been observed in other artificial nanostructures. As a T4-DNA molecule becomes entangled with the nanowire spot-array structure, it frequently has an "M"-shaped conformation, as shown in Figure 3b and c. The unraveling process of the "M"-shaped DNA molecule in the nanowire spot-array structure is completely different from other sieving matrices because of an entanglement point in the middle, the behavior of the electric lines of force, and the strong elastic forces of the DNA molecule. In the nanowire array structure, the unraveling process starts from either ends, *i.e.*, from "M (1.2 s)" to "I (6.0 s)" *via* "Z (2.4 s)" and "J (3.6 s)" shapes in Figure 3b and Supporting Movie 2. On the other hand, the unraveling process in the other sieving matrices, such as the nanowall array structure,[5] starts from the middle part, *i.e.*, from "M" to "I" *via* "U" shapes, as shown in Supporting Movie 3. In Figure 3d–f, we schematically illustrate how the "M"-shaped conformation of the DNA molecule is caused. In the nanowire spot-array structure, there is a nanowire height distribution (see Figure 2e), which results in spatial gaps between nanowires and the cover plate that are around 250 nm on average. In the presence of those spatial gaps, the DNA molecule can exhibit the "M"-shaped conformation as illustrated in Figures 3d–f; the DNA molecule cannot collide with the nanowires due to migration through the gaps, as shown in Figure 3d; the DNA molecule that does not collide still shows Brownian motion in the longitudinal direction coupled with electrophoretic migration, and then it is occasionally caught by the nanowires (Figure 3e); finally, the DNA molecule exhibits the "M"-shaped conformation in Figure 3f. This "M"-shaped conformation in a sparsely ordered post array has been predicted and observed in simulations,[36,37] but our results are the first experimental demonstrations of the existence of the "M"-shaped conformation of DNA molecules. The numerical simulation results theoretically predicted that the "M"-shaped conformation had long-lived entanglements with multiple nanowires, and therefore its

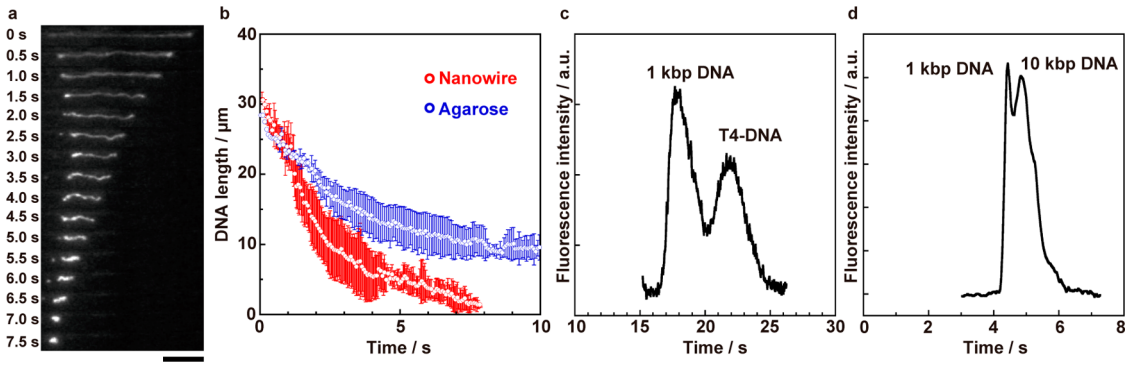

Figure 4. (a) Relaxation process of a well-elongated T4-DNA molecule in the nanowire spot-array structure; scale bar, 10 μm. (b) Plot of T4-DNA length in response to time for the relaxation process of the T4-DNA molecules in the nanowire spot-array structure (red circles) and in the 1% agarose gel (blue circles). Error bars show the standard deviation for a series of measurements ($N = 5$). (c) Separation of 1 kbp DNA (100 ng/μL) and T4-DNA (15 ng/μL). The electropherogram was obtained at 1 mm from the entrance of the microchannel with the nanowire spot-array structure. The applied voltage in the separation channel was 120 V/cm. (d) Separation of 1 kbp DNA (40 ng/μL) and 10 kbp DNA (10 ng/μL). The electropherogram was obtained at 1 mm from the entrance of the microchannel with the denser nanowire array structure. The applied voltage in the separation channel was 217 V/cm.

collision made the distribution of the holdup time longer than that of the classic rope-over-pulley U-, J-, or X-collisions.[38−41] These results highlight that the present nanowire spot-array structure is capable of fully elongating long DNA molecules and causing a long holdup time *via* the unique entanglement events at the desired spatial location of nanowires within the microchannel.

In addition, we determined that the relaxation behavior of T4-DNA within the present nanowire devices is interestingly free-solution-like dynamics. Since the duration of the relaxation time directly determines the frequency of DNA collisions with the nanowire spot-array structure, relaxation time is also a critical factor for controlling the dynamics of DNA molecules. We measured the relaxation time in the nanowire spot-array structure by observing relaxation events in the elongated DNA molecules after switching off the electric field. The time-course relaxation process was observed, as shown in Figure 4a (see also Supporting Movie 4). Figure 4b shows the time series data of DNA length during the relaxation process in the nanowire spot-array structure. Considering the fully stretched length of a T4-DNA molecule as 69.4 μm, we see that the T4-DNA molecules at the starting time are not fully elongated in the structure (35 μm). This is because the DNA molecules start to contract soon after unhooking from the nanowire spot-array structure and the image recording started soon after unraveling from the "U"-shaped conformation. The relaxation process for the nanowire spot-array structure is finished within 7.5 s, which implies DNA molecules show free-solution-like dynamics inside the nanowire spot-array structure. For the sake of comparison, we also show the time series data of the DNA length in 1% agarose gel in Figure 4b. Clearly the relaxation process of DNA molecules in the nanowire spot-array structure is much faster than that in the agarose gel. Since the nanowire density outside the spot-array pattern is much less than that inside, such a low nanowire density area can accelerate the contraction speed of the DNA molecule. Considering the fact that the volume fraction of nanowires within the microchannel is just only 2%, the free-solution-like relaxation dynamics might be somehow understandable. Further theoretical analysis of the relaxation data (Figure S2 in the Supporting Information) has also confirmed that the relaxation dynamics of DNA molecules in the nanowire spot-array structure is free-solution-like behavior. Since the contracted DNA molecules in the nanowire spot-array structure must have a larger gyration radius than their elongated radius, the contracted molecules tend to collide more frequently with the nanowire spot-array structure and show M-collisions, which have a long holdup time and are only possible with the longer DNA. This might cause a significant difference between small and large size DNA molecules regarding the migration speed, which indicates the feasible use of this structure for separating different size DNA molecules.

Separation of DNA Molecules. Figure 4c shows electropherogram data obtained after cross-injection of a mixture of 1 kbp DNA and T4-DNA molecules into the channel with the nanowire structure. The mixture is successfully separated within 30 s by utilizing the nanowire spot-array structure. Figure 4d also shows the separation of the mixture of 1 and 10 kbp DNA molecules within 6 s by utilizing the denser nanowire array structure. Compared to the separation of DNA molecules using nanopillar arrays[2−4] or nanowall arrays,[5] it seems that the DNA separation using the nanowire spot-array structure is more adaptable for the long DNA molecules than for the short DNA molecules, since the long DNA molecules can be elongated significantly due to the nanowire radius relative to the Kuhn length of the DNA molecules; on the other hand, the short DNA molecules will penetrate

the nanowire spot-array structure easily with no elongation.

However there is a dilemma between this successful DNA separation and the free-solution-like DNA dynamics within the nanowire spot-array structure, as discussed in the previous section, because the electrophoretic mobility of different sized DNA molecules is almost constant under free-solution condition, which indicates the intrinsic difficulty for separating them in such an environment. We assumed a key point to interpret such a dilemma as the relatively large effective electric fields within the nanowire spot-array structure, which enhanced the elongation and/or entanglement ("M" shape) of DNA molecules. We calculated the spatial distributions of the electric field for the nanowire spot-array structure to understand the dynamics of DNA molecules within the nanowire spot-array structure (the details of theoretical calculations can be seen in the Supporting Information and Figures S3−S7). We found that the effective electric fields between small nanowires might be larger than those around larger nanopillars due to the penetration of electric lines of force into spacing between small nanowires. Although these static electric field calculations could not fully capture the motions of the negatively charged DNA molecules, qualitatively, DNA molecules should move along the electric lines of force. Therefore they could easily enter and collide with the nanowire spot-array structure more frequently than the large nanopillar structure, which enhances the elongation and/or entanglement ("M" shape) of DNA molecules within the nanowire spot-array structure.

Due to the relatively large electric field within the nanowire spot-array structure, T4-DNA molecules could frequently collide with the nanowire spot-array structure, and the quick (free-solution-like) relaxation would provide them with more chances to interact with the nanowire spot-array structure. These frequent collisions and quick relaxations might cause significant retardation of the electrophoretic mobility of the T4-DNA molecules, resulting in the separation of DNA molecules. To improve separation ability in the nanowire spot-array structure, further theoretical and experimental studies should be undertaken to solve the present mystery in terms of the spatial electrostatic interaction, the rigidity of nanowires, the fluid dynamics within nanowires, and the surface charge distributions at the nanowire surface.

CONCLUSION

In summary, we have demonstrated that a precisely positioned sublithographic-scale nanowire array structure embedded in a microchannel on a fused silica substrate could be used to manipulate the dynamics of a single long DNA molecule and to separate different DNA molecules. Our experimental results highlighted the great potential that the nanowire spot-array structure has for elongation and separation of biomolecules and also demonstrated its superiority to the conventional gel matrix in terms of spatial controllability within a microchannel, which is essential to further integrate the array structure with other functionalities using neighboring nanostructures for sensing and identifying biomolecule species (Figure S8 in the Supporting Information). Further theoretical and experimental studies are desirable to improve the manipulation of DNA molecules in the nanowire structure and enhance their separation; this should include such considerations as the effects of position, density, surface charge distribution, and rigidity of the nanowires. The spatial controllability of sublithographic-scale nanowires within microchannels that we have demonstrated here offers a flexible platform to manipulate and separate DNA molecules and moves researchers toward the goal of further integration with other nanostructures for sensing biomolecules including DNA sequencing.

METHODS

Nanowire Chip Fabrication. The nanowire chips were fabricated on fused silica substrates (Crystal Base Co.). First, a 250 nm thick Cr layer was deposited on the substrate by RF sputtering (SVC-700LRF, Sanyu Denshi) as drawn in Figure 1a-1; the layer was a mask for the dry etching process to fabricate a microchannel. Positive photoresist (TSMR V50, Tokyo Ohka Kogyo Co.) was spin-coated on the Cr layer, and then the microchannel pattern with a width of 25 μm was formed by photolithography (Figure 1a-2). After development of the resist, the patterned area of Cr was etched by immersing in Cr etchant (H_2O/$Ce(NH_4)_2(NO_3)_6$/$HClO_4$, 85:10:5 by weight percent) for 5 min. The microchannel was formed by reactive ion etching (RIE-10NR, Samco Co.) under CF_4 gas ambient (Figure 1a-3). The depth of the microchannel was controlled to 2 μm, which is larger than the radius of gyration of T4-DNA. Inlet and outlet *via* holes of 1.5 mm diameter for the microchannel were formed with an ultrasonic driller (SOM-121, Shinoda Co.). The metal catalyst was patterned to define the spatial position of nanowires within the microchannel. A 10 nm thick Cr layer was deposited within the microchannel (Figure 1a-4). Positive resist (ZEP520 A7, Zeon Corp.) was coated on the microchannel by spin-coating (Figure 1a-5), and then the hexagonal array pattern was drawn by electron beam lithography (SPG-724, Sanyu Electron Co.) in Figure 1a-6. After developing the resist, the Cr layer of the array pattern was removed by Cr etchant. A 3 nm diameter Au metal catalyst for nanowire growth was deposited within the microchannel by sputtering (Figure 1a-7). Then the resist was lifted off using dimethylformamide followed by acetone. Next, the Cr layer was lifted off by Cr etchant. The presence of a thicker Cr layer on the outside of microchannel allowed the Au metal catalyst pattern to be retained only within the microchannel (Figure 1a-8). The well-patterned catalyst array was used to fabricate spatially patterned SnO_2 nanowires by pulse laser deposition (Figure 1a-9). Details of the nanowire fabrication conditions are given elsewhere.[30,42−50] Finally the microchannel was sealed using a 130 μm thick fused silica cover plate (Crystal Base Co.) according to the literature method (Figure 1a-10).[4,5]

DNA Observations in the Nanowire Spot-Array Structure. Single DNA molecule observations in the nanowire spot-array structure were performed using T4-DNA molecules (166 kbp; Nippon Gene Co., Ltd.) stained with the dye YOYO-1 (Invitrogen) at a dye-to-base pair ratio of 1:5. For DNA separation experiments, DNA fragments of 1 kbp (NoLimits, Fermentas) and T4-DNA were stained with YOYO-1 at a dye-to-base pair ratio of 1:10. A concentrated buffer solution (5× TBE; 445 mM Tris-borate and 10 mM EDTA, pH 8.2, Sigma-Aldrich, Inc.) containing 10 mM dithiothreitol (DTT, Sigma-Aldrich, Inc.) was used to reduce photobleaching of the DNA molecules stained with YOYO-1. An inverted fluorescent microscope (Eclipse TE-300, Nikon) equipped with a high-voltage sequencer (HVS448-1500, Lab Smith) was used to apply the electric fields, and a 488 nm wavelength laser (FLS-488-20, Sigma Koki Co., Ltd.) with 20 mW output power was used to observe the fluorescently stained DNA molecules; fluorescence images were captured with an EB-CCD camera (C7190-43, Hamamatsu Photonics K.K.) through a 100×/1.40 NA objective lens (Nikon). The images were recorded on a DV tape (DSR-11, Sony) and then analyzed by image-processing software (Cosmos 32, Library).

DNA Observations in the Agarose Gel. T4-DNA molecules, stained with YOYO-1 at a dye-to-base pair ratio of 1:5, were observed in polydimethylsiloxane (PDMS) microchannels (width and height were 650 and 50 μm, respectively), which were filled with the 1% agarose gel (Pulsed Field Certified Agarose, Bio-Rad Laboratories, Inc.) in 5× TBE. Elongation of T4-DNA molecules in the gel was performed by applying an electric field of 5 V/cm for a few minutes; relaxation of T4-DNA molecules was observed, through the 100×/1.40 NA objective lens, soon after switching off the electric field in the inverted fluorescent microscope (Eclipse TE-300) equipped with the high-voltage sequencer (HVS448-1500), the 488 nm wavelength laser (FLS-488-20), and the EB-CCD camera (C7190-43). The images were recorded on a DV tape (DSR-11) and then analyzed by image-processing software (Cosmos 32).

Conflict of Interest: The authors declare no competing financial interest.

Acknowledgment. This research was supported by the Japan Society for the Promotion of Science (JSPS) through its "Funding Program for World-Leading Innovative R&D on Science and Technology (FIRST Program)" and partly supported by Nanotechnology Platform Program (Molecule and Material Synthesis) of the Ministry of Education, Culture, Sports, Science and Technology (MEXT), Japan. Thanks are extended to Dr. Y. Okamoto and Dr. D. Onoshima, both of Nagoya University, for valuable discussions.

Supporting Information Available: (1) Dielectric breakdown of Si substrate with the 60 nm thick SiO_2 layer; (2) theoretical analysis of the relaxation data; (3) electric field calculation for the nanowire array; (4) nanowires embedded in a nanopore channel; and (5) movies. This material is available free of charge *via* the Internet at http://pubs.acs.org.

REFERENCES AND NOTES

1. Volkmuth, W. D.; Austin, R. H. DNA Electrophoresis in Microlithographic Arrays. *Nature* **1992**, *358*, 600–602.
2. Kaji, N.; Tezuka, Y.; Takamura, Y.; Ueda, M.; Nishimoto, T.; Nakanishi, H.; Horiike, Y.; Baba, Y. Separation of Long DNA Molecules by Quartz Nanopillar Chips under a Direct Current Electric Field. *Anal. Chem.* **2004**, *76*, 15–22.
3. Yasui, T.; Kaji, N.; Ogawa, R.; Hashioka, S.; Tokeshi, M.; Horiike, Y.; Baba, Y.DNA Separation by Square Patterned Nanopillar Chips.*Micro Total Analysis Systems 2007*; Chemical and Biological Microsystems Society, 2007; Vol. 2, pp 1207−1209.
4. Yasui, T.; Kaji, N.; Mohamadi, M. R.; Okamoto, Y.; Tokeshi, M.; Horiike, Y.; Baba, Y. Electroosmotic Flow in Microchannels with Nanostructures. *ACS Nano* **2011**, *5*, 7775–7780.
5. Yasui, T.; Kaji, N.; Ogawa, R.; Hashioka, S.; Tokeshi, M.; Horiike, Y.; Baba, Y. DNA Separation in Nanowall Array Chips. *Anal. Chem.* **2011**, *83*, 6635–6640.
6. Han, J.; Craighead, H. G. Separation of Long DNA Molecules in a Microfabricated Entropic Trap Array. *Science* **2000**, *288*, 1026–1029.
7. Fu, J.; Yoo, J.; Han, J. Molecular Sieving in Periodic Free-Energy Landscapes Created by Patterned Nanofilter Arrays. *Phys. Rev. Lett.* **2006**, *97*, 018103.
8. Fu, J.; Schoch, R. B.; Stevens, A. L.; Tannenbaum, S. R.; Han, J. A Patterned Anisotropic Nanofluidic Sieving Structure for Continuous-Flow Separation of DNA and Proteins. *Nat. Nanotechnol.* **2007**, *2*, 121–128.
9. Mao, P.; Han, J. Massively-Parallel Ultra-High-Aspect-Ratio Nanochannels as Mesoporous Membranes. *Lab Chip* **2009**, *9*, 586–591.
10. Park, S. G.; Olson, D. W.; Dorfman, K. D. DNA Electrophoresis in a Nanofence Array. *Lab Chip* **2012**, *12*, 1463–1470.
11. Li, W. L.; Tegenfeldt, J. O.; Chen, L.; Austin, R. H.; Chou, S. Y.; Kohl, P. A.; Krotine, J.; Sturm, J. C. Sacrificial Polymers for Nanofluidic Channels in Biological Applications. *Nanotechnology* **2003**, *14*, 578–583.
12. Cross, J. D.; Strychalski, E. A.; Craighead, H. G. Size-Dependent DNA Mobility in Nanochannels. *J. Appl. Phys.* **2007**, *102*, 024701.
13. Pennathur, S.; Baldessari, F.; Santiago, J. G.; Kattah, M. G.; Steinman, J. B.; Utz, P. J. Free-Solution Oligonucleotide Separation in Nanoscale Channels. *Anal. Chem.* **2007**, *79*, 8316–8322.
14. Doyle, P. S.; Bibette, J.; Bancaud, A.; Viovy, J. L. Self-Assembled Magnetic Matrices for DNA Separation Chips. *Science* **2002**, *295*, 2237.
15. Tabuchi, M.; Ueda, M.; Kaji, N.; Yamasaki, Y.; Nagasaki, Y.; Yoshikawa, K.; Kataoka, K.; Baba, Y. Nanospheres for DNA Separation Chips. *Nat. Biotechnol.* **2004**, *22*, 337–340.
16. Zeng, Y.; Harrison, D. J. Self-Assembled Colloidal Arrays as Three-Dimensional Nanofluidic Sieves for Separation of Biomolecules on Microchips. *Anal. Chem.* **2007**, *79*, 2289–2295.
17. Nazemifard, N.; Bhattacharjee, S.; Masliyah, J. H.; Harrison, D. J. DNA Dynamics in Nanoscale Confinement under Asymmetric Pulsed Field Electrophoresis. *Angew. Chem., Int. Ed.* **2010**, *49*, 3326–3329.
18. Schoch, R. B.; Han, J. Y.; Renaud, P. Transport Phenomena in Nanofluidics. *Rev. Mod. Phys.* **2008**, *80*, 839–883.
19. Salieb-Beugelaar, G. B.; Dorfman, K. D.; van den Berg, A.; Eijkel, J. C. Electrophoretic Separation of DNA in Gels and Nanostructures. *Lab Chip* **2009**, *9*, 2508–2523.
20. Kaji, N.; Okamoto, Y.; Tokeshi, M.; Baba, Y. Nanopillar, Nanoball, and Nanofibers for Highly Efficient Analysis of Biomolecules. *Chem. Soc. Rev.* **2010**, *39*, 948–956.
21. Dorfman, K. D. DNA Electrophoresis in Microfabricated Devices. *Rev. Mod. Phys.* **2010**, *82*, 2903–2947.
22. Tsutsui, M.; Taniguchi, M.; Kawai, T. Single-Molecule Identification *via* Electric Current Noise. *Nat. Commun.* **2010**, *1*, 138.
23. Tsutsui, M.; Taniguchi, M.; Yokota, K.; Kawai, T. Identifying Single Nucleotides by Tunnelling Current. *Nat. Nanotechnol.* **2010**, *5*, 286–290.
24. Araki, N.; Aydil, E. S.; Dorfman, K. D. Collision of a Long DNA Molecule with an Isolated Nanowire. *Electrophoresis* **2010**, *31*, 3675–3680.
25. Hochbaum, A. I.; Fan, R.; He, R.; Yang, P. Controlled Growth of Si Nanowire Arrays for Device Integration. *Nano Lett.* **2005**, *5*, 457–460.
26. Jung, M. H.; Lee, H. Selective Patterning of ZnO Nanorods on Silicon Substrates Using Nanoimprint Lithography. *Nanoscale Res. Lett.* **2011**, *6*, 159.
27. Wang, X. D.; Summers, C. J.; Wang, Z. L. Large-Scale Hexagonal-Patterned Growth of Aligned ZnO Nanorods for Nano-Optoelectronics and Nanosensor Arrays. *Nano Lett.* **2004**, *4*, 423–426.
28. Greyson, E. C.; Babayan, Y.; Odom, T. W. Directed Growth of Ordered Arrays of Small-Diameter ZnO Nanowires. *Adv. Mater.* **2004**, *16*, 1348–1352.
29. Fan, H. J.; Werner, P.; Zacharias, M. Semiconductor Nanowires: From Self-Organization to Patterned Growth. *Small* **2006**, *2*, 700–717.

30. Klamchuen, A.; Yanagida, T.; Kanai, M.; Nagashima, K.; Oka, K.; Rahong, S.; Gang, M.; Horprathum, M.; Suzuki, M.; Hidaka, Y.; *et al*. Study on Transport Pathway in Oxide Nanowire Growth by Using Spacing-Controlled Regular Array. *Appl. Phys. Lett.* **2011**, *99*, 193105.
31. Jensen, L. E.; Bjork, M. T.; Jeppesen, S.; Persson, A. I.; Ohlsson, B. J.; Samuelson, L. Role of Surface Diffusion in Chemical Beam Epitaxy of Inas Nanowires. *Nano Lett.* **2004**, *4*, 1961–1964.
32. Bustamante, C.; Marko, J. F.; Siggia, E. D.; Smith, S. Entropic Elasticity of Lambda-Phage DNA. *Science* **1994**, *265*, 1599–1600.
33. Perkins, T. T.; Smith, D. E.; Larson, R. G.; Chu, S. Stretching of a Single Tethered Polymer in a Uniform-Flow. *Science* **1995**, *268*, 83–87.
34. Bakajin, O. B.; Duke, T. A. J.; Chou, C. F.; Chan, S. S.; Austin, R. H.; Cox, E. C. Electrohydrodynamic Stretching of DNA in Confined Environments. *Phys. Rev. Lett.* **1998**, *80*, 2737–2740.
35. Mannion, J. T.; Reccius, C. H.; Cross, J. D.; Craighead, H. G. Conformational Analysis of Single DNA Molecules Undergoing Entropically Induced Motion in Nanochannels. *Biophys. J.* **2006**, *90*, 4538–4545.
36. Sevick, E. M.; Williams, D. R. M. Long-Lived States in Electrophoresis: Collision of a Polymer Chain with Two or More Obstacles. *Europhys. Lett.* **2001**, *56*, 529–535.
37. Cho, J.; Dorfman, K. D. Brownian Dynamics Simulations of Electrophoretic DNA Separations in a Sparse Ordered Post Array. *J. Chromatogr. A* **2010**, *1217*, 5522–5528.
38. Volkmuth, W. D.; Duke, T.; Wu, M. C.; Austin, R. H.; Szabo, A. DNA Electrodiffusion in a 2D Array of Posts. *Phys. Rev. Lett.* **1994**, *72*, 2117–2120.
39. Nixon, G. I.; Slater, G. W. DNA Electrophoretic Collisions with Single Obstacles. *Phys. Rev. E* **1994**, *50*, 5033–5038.
40. Masubuchi, Y.; Oana, H.; Akiyama, T.; Matsumoto, M.; Doi, M. Dynamics of a DNA Molecule Hanging over an Obstacle in Gel-Electrophoresis. *J. Phys. Soc. Jpn.* **1995**, *64*, 1412–1420.
41. Randall, G. C.; Doyle, P. S. Collision of a DNA Polymer with a Small Obstacle. *Macromolecules* **2006**, *39*, 7734–7745.
42. Klamchuen, A.; Yanagida, T.; Nagashima, K.; Seki, S.; Oka, K.; Taniguchi, M.; Kawai, T. Crucial Role of Doping Dynamics on Transport Properties of Sb-Doped SnO_2 Nanowires. *Appl. Phys. Lett.* **2009**, *95*, 053105.
43. Nagashima, K.; Yanagida, T.; Tanaka, H.; Seki, S.; Saeki, A.; Tagawa, S.; Kawai, T. Effect of the Heterointerface on Transport Properties of *in situ* Formed MgO/Titanate Heterostructured Nanowires. *J. Am. Chem. Soc.* **2008**, *130*, 5378–5382.
44. Oka, K.; Yanagida, T.; Nagashima, K.; Tanaka, H.; Kawai, T. Nonvolatile Bipolar Resistive Memory Switching in Single Crystalline NiO Heterostructured Nanowires. *J. Am. Chem. Soc.* **2009**, *131*, 3434–3435.
45. Oka, K.; Yanagida, T.; Nagashima, K.; Tanaka, H.; Seki, S.; Honsho, Y.; Ishimaru, M.; Hirata, A.; Kawai, T. Specific Surface Effect on Transport Properties of NiO/MgO Heterostructured Nanowires. *Appl. Phys. Lett.* **2009**, *95*, 133110.
46. Nagashima, K.; Yanagida, T.; Oka, K.; Taniguchi, M.; Kawai, T.; Kim, J. S.; Park, B. H. Resistive Switching Multistate Nonvolatile Memory Effects in a Single Cobalt Oxide Nanowire. *Nano Lett.* **2010**, *10*, 1359–1363.
47. Oka, K.; Yanagida, T.; Nagashima, K.; Kawai, T.; Kim, J. S.; Park, B. H. Resistive-Switching Memory Effects of NiO Nanowire/Metal Junctions. *J. Am. Chem. Soc.* **2010**, *132*, 6634–6635.
48. Klamchuen, A.; Yanagida, T.; Kanai, M.; Nagashima, K.; Oka, K.; Kawai, T.; Suzuki, M.; Hidaka, Y.; Kai, S. Role of Surrounding Oxygen on Oxide Nanowire Growth. *Appl. Phys. Lett.* **2010**, *97*, 073114.
49. Nagashima, K.; Yanagida, T.; Oka, K.; Kanai, M.; Klamchuen, A.; Kim, J. S.; Park, B. H.; Kawai, T. Intrinsic Mechanisms of Memristive Switching. *Nano Lett.* **2011**, *11*, 2114–2118.
50. Klamchuen, A.; Yanagida, T.; Kanai, M.; Nagashima, K.; Oka, K.; Seki, S.; Suzuki, M.; Hidaka, Y.; Kai, S.; Kawai, T. Dopant Homogeneity and Transport Properties of Impurity-Doped Oxide Nanowires. *Appl. Phys. Lett.* **2011**, *98*, 053107.